Proceeding of the 2004 American Control Conference
Boston, Massachusetts June 30 - July 2, 2004

Adaptive control of a flexible-link mechanism using an energy-based approach

Alberto Trevisani and Maria Elena Valcher

***Abstract*— The aim of any control scheme for a flexible-link mechanism is that of ensuring that the controlled system performs a fast and accurate positioning while exhibiting small vibrations. Aiming at achieving these goals, in this paper an adaptive controller is proposed for a four-bar flexible link mechanism. The controller is obtained by superposing a PD position controller and an adaptive proportional vibration controller. The position controller is a priori tuned, basing on the physical features of the flexible mechanism. The vibration controller, instead, is a proportional controller whose gains are adaptively tuned to ensure good performances even when working conditions change and abrupt disturbances affect the system functioning. The controlled-system stability is formally proved by means of an energy-based approach. Moreover, the controller performances are illustrated by means of simulations and compared to the performances of "analogous" non-adaptive control schemes.**

I. INTRODUCTION

Several contributions have appeared in the literature concerning the modeling, analysis and control of flexible-link mechanisms and manipulators. As far as modeling is concerned, a widespread assumption consists in defining the total motion of the system through the superposition of a large-amplitude rigid-body motion and a small-amplitude elastic deformation (vibration). Accurate dynamic models must include coupling terms representing not only the effect of the rigid-body motion on the elastic motion, but also the effect of the elastic motion on the rigid-body motion [5].

When addressing the synthesis of position and vibration controllers, however, the complexity of the fully coupled analytical models makes real-time model-based control a difficult task. Linear control schemes have been chiefly employed with varying degrees of success. In particular, linear quadratic optimal control strategies have been adopted to control both single-link [12] and multi-body [1] systems. In these works, the system dynamics has been described by means of approximate linear state-space models, and the control action has been expressed as a state-feedback. Since direct measurement of all the state variables of a flexible-link system is almost ever impossible, in order to practically employ such control strategies one may design a state observer. However, a sufficiently accurate observer would generally need employing a non-linear dynamic model, which in turn increases the difficulties in the design process and makes real-time computations too expensive.

An alternative choice consists in designing a dynamic output feedback compensator as, for instance, in [9]. The main drawback of this solution, however, is that the controller complexity may significantly increase as the system model accuracy, and hence the dimensions, increase. For these reasons, simpler and more traditional control strategies, based on the use of standard regulators, have also been proposed.

PD controllers are the basic components of the scheme proposed to control the tip position of a single-link flexible mechanism in [8]. In [3] partially uncoupled position and vibration control of a flexible four-bar linkage with all the links flexible is achieved making use of independent PID-like and proportional regulators.

Admittedly, model-based control techniques, as well as those just employing standard regulators, exhibit a number of drawbacks. In particular, the latter yields the problem of performing an appropriate tuning of the regulator parameters, which is suitable for all the operating conditions. The former, on the other hand, typically involves using high-order controllers which are difficult to implement and extremely sensitive to parameter uncertainties; moreover, if the system model the controller is based upon is obtained by truncation, one must cope with the additional problem of control and observation spillover.

To overcome these difficulties, an energy-based control design technique has been proposed [4]. Being model-independent, this approach allows resorting to quite simple controller structures, as, for instance, PID controllers, meanwhile guaranteeing robust performances. Though stability may always be ensured even by assigning constant values to the controller parameters, the controlled system performances may significantly degrade as a result of model uncertainty, changing working conditions or abrupt disturbances affecting the system functioning. So, a solution may be adaptively tuning the controller parameters. Adaptive control techniques have been frequently applied to the control of flexible-link mechanisms [7], [11]. On the other hand, in [6] a solution has been proposed, combining the advantages of the energy-based approach with those of regulators with adaptively changing parameters.

In this paper we consider a four-bar planar mechanism with all the links flexible except for the ground link, and design a controller which ensures that the resulting controlled flexible-link mechanism performs a fast and accurate positioning while exhibiting small vibrations. The

A.Trevisani is with the Dipartimento di Innovazione Meccanica e Gestionale, Università di Padova, viale Venezia 1, Padova, Italy, alberto.trevisani@unipd.it

M.E.Valcher is with the Dipartimento di Ingegneria dell'Informazione, via Gradenigo 6/B, Università di Padova, Padova, Italy, meme@dei.unipd.it

controlled variables are the crank angle and the curvatures of the links. The control scheme can be thought of as the superposition of two separated position and vibration controllers. The position controller consists of a PD regulator whose parameters may be a priori tuned. The vibration controller consists of proportional controllers whose gains are adaptively tuned depending both on the link curvatures, and, for stability reasons, on the crank angular position and velocity.

Basically, the proposed scheme might be regarded as an “adaptive-type” enhancement of the scheme proposed in [3]. The introduction of an adaptive law for the gains of the vibration controller aims at simplifying parameter tuning and, above all, improving the system performances when major vibrational phenomena take place. Differently from [3], a stability analysis of the resulting control scheme is performed in this work. The proof of simple stability is obtained by resorting to a model-independent energy-based approach, as in [6]. However, compared to [6], a more intuitive control law has been adopted.

The aforementioned system model has allowed implementing the simulation environment in which the controller performances have been assessed. The performances of the proposed scheme have been compared with both those of a similar scheme, but lacking vibration controllers, and, which is more substantial, with those of an identical, but non-adaptive scheme. The results achieved prove the effectiveness of the controller, especially when abrupt disturbances affect the system functioning.

II. DYNAMIC MODEL

A synthetic description of the mathematical model adopted to reproduce the dynamic response of the studied system is provided in this section, where only the most relevant equations are reported. The model, which is valid for any chain of flexible bodies, is based on the one proposed in [5]. The equations of motion are obtained through the direct application of the principle of virtual work. Moreover, the total motion of each flexible link is separated into the large rigid-body motion of an equivalent rigid-link system (ERLS) and the small elastic displacements of any point with respect to the ERLS itself. Finally, so as to get a model with a finite number of degrees of freedom, the links are subdivided into finite elements. The model ensures accurate simulation of the system dynamic behavior because inertia coupling between rigid-body motion and vibrations, as well as the effects of the chief geometric and inertial non-linearities of the physical system, are accounted for.

In the adopted model, the following kinematic definitions are employed:

• $\mathbf{r}_i$ and $\mathbf{u}_i$ are the vectors of the positions of the nodes in the ith element of the ERLS and of their elastic displacements, respectively. The sum of these vectors provides the global motion of the nodes of the ith element.

• $\mathbf{p}_i$ is the position vector of a generic point of the ith element;

• $\mathbf{q}$ is the vector containing the generalized coordinates of the ERLS.

All the vectors considered are defined in a common fixed reference frame, a local reference frame following the motion of the ERLS is also defined for each element so as to simplify the use of finite element techniques.

The governing equations of motion, obtained by applying the principle of virtual work, are:

$$\begin{aligned}&\textstyle\sum_i \int_{V_i} \delta\mathbf{p}_i^T \ddot{\mathbf{p}}_i \ \rho_i \ d\nu + \sum_i \int_{V_i} \delta\boldsymbol{\varepsilon}_i^T \mathbf{D}_i \ \boldsymbol{\varepsilon}_i \ d\nu = \\ &= \textstyle\sum_i \int_{V_i} \delta\mathbf{p}_i^T \mathbf{g} \ \rho_i \ d\nu + (\delta\mathbf{u}^T + \delta\mathbf{r}^T)\mathbf{f}.\end{aligned} \tag{1}$$

In the equation above the total virtual work is split into the elemental contributions, i.e. into the element volumes V_i, and dumping is initially neglected. As for the meaning of the symbols, $\boldsymbol{\varepsilon}_i$, $\mathbf{D}_i$ and ρ_i are respectively the strain vector, the stress-strain matrix and the mass density for the ith element, $\mathbf{g}$ is the gravity acceleration vector, $\mathbf{f}$ is the vector of the concentrated external forces and torques, and $\delta\mathbf{u}$ and $\delta\mathbf{r}$ refer to the virtual displacements of all the nodes of the model.

The following interpolations are employed for the virtual displacement and real acceleration of a generic point

$$\begin{aligned}\delta\mathbf{p}_i &= \mathbf{R}_i\mathbf{N}_i\mathbf{T}_i \ \delta\mathbf{r}_i + \mathbf{R}_i\mathbf{N}_i\mathbf{T}_i \ \delta\mathbf{u}_i \\ \ddot{\mathbf{p}}_i &= \mathbf{R}_i\mathbf{N}_i\mathbf{T}_i\ddot{\mathbf{r}}_i + \mathbf{R}_i\mathbf{N}_i\mathbf{T}_i\ddot{\mathbf{u}}_i + 2(\dot{\mathbf{R}}_i\mathbf{N}_i\mathbf{T}_i + \mathbf{R}_i\mathbf{N}_i\dot{\mathbf{T}}_i)\dot{\mathbf{u}}_i\end{aligned}$$

where

• $\mathbf{T}_i$ is a matrix describing the transformation from the global to the local reference frame of the ith element and $\mathbf{R}_i$ is the local-to-global rotation matrix;

• $\mathbf{N}_i$ is the shape function matrix of the ith element and is defined in the local frame.

As for the real and virtual strains, the following expressions hold in the local moving frame:

$$\boldsymbol{\varepsilon}_i = \mathbf{B}_i\mathbf{T}_i\mathbf{u}_i \tag{2}$$

$$\delta\boldsymbol{\varepsilon}_i = \mathbf{B}_i \ \delta\mathbf{T}_i\mathbf{u}_i + \mathbf{B}_i\mathbf{T}_i \ \delta\mathbf{u}_i \tag{3}$$

where $\mathbf{B}_i(x_i, y_i, z_i)$ is the strain-displacement matrix.

Because the nodal elastic virtual displacements ($\delta\mathbf{u}$) and the nodal virtual displacements of the ERLS ($\delta\mathbf{r}$) are completely independent of each other, from the reported basic relations it is possible to get this final expression of the system equations of motion:

$$\begin{bmatrix} \mathbf{M}_{in} & (\mathbf{MS})_{in} \\ (\mathbf{S}^T\mathbf{M})_{in} & \mathbf{S}^T\mathbf{MS} \end{bmatrix} \begin{bmatrix} \ddot{\mathbf{u}}_{in} \\ \ddot{\mathbf{q}} \end{bmatrix} = \begin{bmatrix} \mathbf{t}_{in} \\ \mathbf{S}^T\mathbf{t} \end{bmatrix}. \tag{4}$$

In the equation above, the vector $\mathbf{t} = \mathbf{t}(\mathbf{u}, \dot{\mathbf{u}}, \mathbf{q}, \dot{\mathbf{q}})$ accounts for all the forces excluding those directly related to the second derivatives of the generalized coordinates. It also includes damping forces because simple Rayleigh damping is introduced in the equations of motion. Moreover, $\mathbf{M}$ is the matrix obtained assembling the mass matrices of the elements and $\mathbf{S}$ is the ERLS sensitivity coefficient matrix for all the nodes, which is obviously an explicit function of $\mathbf{q}$. As for the meaning of the subscript *in*, it is a consequence of the fact that the position of the ERLS is defined forcing to zero a number of elastic displacements equal to the number of generalized coordinates of the ERLS. Only the nodal elastic displacements which are not forced to zero, and the corresponding matrix elements, are considered in equation (6), and they are indicated by the subscript *in*.

The correctness of the adopted model has been experimentally verified in [5] and [2] with respect to two different flexible-link planar mechanisms.

III. TEST CASE

The test case considered to evaluate the performances of the control scheme presented in the next section is a planar four-bar mechanism, with all the links flexible except for one ("link 0") (see [3]). In this work it is assumed that the mechanism is unaffected by gravity. Fig. 1 shows the scheme of the mechanism and the position of the nodes of the elements with which the links are modeled in the finite element analysis.

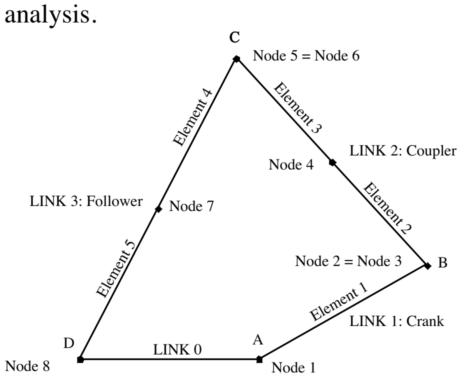

Fig. 1 Scheme of the four-bar linkage.

All the links are supposed to be straight and slender steel bars with a square cross section. All the link lengths are different to make it possible to distinguish the link vibration frequencies in the system response. Moreover, the mechanism is supposed to be driven by a servomotor connected to the crank at joint A. The generalized coordinate q is the ERLS crank angle at the drive shaft (joint A), while the elastic degree of freedom, forced to zero to define the position of the ERLS, is the displacement in the horizontal direction at joint C.

IV. CONTROL DESIGN

In this paper, an energy-based [4], [6] control design technique is employed. The elementary energy relationship it is based upon, and the Lyapunov-like technique adopted for testing its stabilizing properties, ensure a simple implementation and robust performances. As in [3], the control scheme makes use of the crank angle and the curvatures of the links, which represent, at the same time, the to-be-controlled and the measured variables, and produces, as control input, the torque applied to the crank and generated by the servomotor. The controller structure does not require flexible modes reconstruction, thus ruling out control and observation spillover problems.

The controller is obtained by superposing a position controller and a vibration controller. The former is a priori tuned, on the basis of the physical features of the flexible mechanism. It consists of a PD controller which depends on the crank angle alone. The latter, instead, is a proportional controller whose gains are adaptively tuned to ensure good performances even when working conditions change and abrupt disturbances affect the system functioning.

In order to specify the controller structure, we need to preliminarily introduce some notation:

- $\theta(t)$ represents the mechanism crank angle at time instant t (θ is the sum of the generalized coordinate q and the elastic rotation at node 1);

- $\dot{\theta}(t)$ represents the crank angular velocity at time t;

- θ_d represents the desired crank angle. The analysis carried on in this paper concerns both regulation problems and tracking problems with reference signal which is piecewise constant with sufficiently distant switching times (for instance, a square wave);

- $\tau(t)$ is the torque produced by the servomotor and applied to the crank at joint A at time instant t;

- $C_j(t)$ is the curvature of the jth link of length L_j, $j = 1, 2, 3$, measured at time t, at a fixed distance $s_j L_j$ from the first node (the one having lowest number in Fig. 1) of the link. The curvature C_j can be evaluated from (2), and the value of each s_j should be chosen in order to maximize the signal-to-noise ratio.

The adaptive PD controller that provides the torque function in terms of $\theta(t)$, $\dot{\theta}(t)$ and $C_j(t)$, $j = 1, 2, 3$, is described by the following law

$$\tau(t) = k_p(\theta_d - \theta(t)) - k_d\dot{\theta}(t) - \sum_{j=1}^{3} k_j(t)C_j(t), \qquad (5)$$

where k_p and k_d are positive constant parameters, while $k_j(t)$, $j = 1, 2, 3$, is a time-varying parameter whose dynamics is described by the adaptive differential law:

$$\dot{k}_j(t) = \alpha_j C_j(t)\dot{\theta}(t) - \beta_j k_j(t) - \gamma_j(\theta_d - \theta(t))^2 k_j(t). \quad (6)$$

α_j, β_j and γ_j are positive parameters. Equation (6) deserves some comments. The adaptive gain $k_j(t)$ depends on the tracking error $\theta_d - \theta(t)$ and its derivative $-\dot{\theta}(t)$ as well as on the curvature of the jth link $C_j(t)$. The dependence of $\dot{k}_j(t)$ on the product $C_j(t)\dot{\theta}(t)$ is not intuitive, but its effectiveness will be proved both by theoretical means and via simulation.

Of course, the gain $k_j(t)$, and hence the corresponding proportional action, should go to zero when the vibrations have been suppressed and the desired angular position has been steadily reached by the crank. In practice, however, noise and steady-state offset problems may lead to increasing values of the gain $k_j(t)$ and hence to torque values out of the acceptable range, thus affecting the system stability [7]. The term $-\beta_j k_j(t)$ has been introduced just to prevent this problem. Notice that the adaptive control law (5)-(6) is simply based on the measurement of $\theta(t)$, $\dot{\theta}(t)$ and $C_j(t)$, $j = 1, 2, 3$, which are easy to get on a physical system. Thus the control law is easy to implement.

V. STABILITY ANALYSIS

In this section we will prove that by applying the control law (5)-(6) in order to pursue the control objective of rotating the crank angle to the desired position θ_d, meanwhile suppressing the system vibrations, we can ensure the stability of the resulting controlled system (i.e., $\theta \rightarrow \theta_d$ and $C_1, C_2, C_3 \rightarrow 0$). It is worth remarking that this same stability analysis immediately extends to the case of tracking problems when the desired angular position θ_d is a piece-wise constant function and the distance between one switching time and the following one is large enough if compared to the settling time.

For the sake of simplicity, we assume that neither gravity nor friction or damping affect the system functioning.

Let $E_k(t)$ and $E_p(t)$ denote the total kinetic energy and the potential (elastic) energy of the controlled system, respectively, at the time instant t, and consider the following Lyapunov function:

$$V(t) = E_k(t) + E_p(t) + \frac{k_p}{2}(\theta_d - \theta(t))^2 + \sum_{j=1}^{3} \frac{k_j^2(t)}{2\alpha_j}.$$

By taking the derivative of $V(t)$ one gets

$$\begin{aligned} \dot{V}(t) &= \dot{E}_k(t) + \dot{E}_p(t) - k_p(\theta_d - \theta(t))\dot{\theta}(t) \\ &+ \sum_{j=1}^{3} \frac{k_j(t)\dot{k}_j(t)}{\alpha_j}. \end{aligned} \tag{7}$$

As damping, friction and gravity have been neglected, the total change in the system energy $E_k(t) + E_p(t)$ must coincide with the total work done by the motor torque, and hence, can be expressed as follows:

$$[E_k(t)+E_p(t)] - [E_k(0)+E_p(0)] = \int_0^t \dot{\theta}(\sigma)\tau(\sigma)d\sigma. \tag{8}$$

Consequently, by taking the time derivative of both sides of (8) one gets:

$$\dot{E}_k(t) + \dot{E}_p(t) = \dot{\theta}(t)\tau(t). \tag{9}$$

By replacing (9) in (7) one obtains:

$$\dot{V}(t) = \dot{\theta}(t)\tau(t) - k_p(\theta_d - \theta(t))\dot{\theta}(t) + \sum_{j=1}^{3} \frac{k_j(t)\dot{k}_j(t)}{\alpha_j}. \tag{10}$$

Then, by replacing $\tau(t)$ and $k_j(t)$ with their expressions given in (5) and (6) respectively, it follows that

$$\dot{V}(t) = -k_d\dot{\theta}(t)^2 - \sum_{j=1}^{3} \frac{\beta_j}{\alpha_j} k_j^2(t) - \sum_{j=1}^{3} \frac{\gamma_j}{\alpha_j}(\theta_d - \theta(t))^2 k_j^2(t) \tag{11}$$

$\dot{V}(t)$ only takes non-positive values, which proves that the energy along the system trajectories cannot increase. Moreover, as $V(t)$ is a continuous function of $k_j(t)$ and $0 \leq V(t) \leq V(0)$, $\forall\ t \geq 0$, $k_j(t)$ is bounded. So, the resulting controlled system is energy-dissipative and hence stable.

Remark Notice that $\frac{k_p}{2}(\theta_d - \theta(t))^2 \leq V(t) \leq V(0), \forall\ t \in \mathbb{R}_+$. This ensures that the error $\theta_d - \theta(t)$ is always bounded. Moreover, all adaptive controller parameters are bounded.

VI. NUMERICAL RESULTS

Table 1 reports the mechanical characteristics of the mechanism to which the theory developed in the foregoing sections has been applied. Damping has been introduced to achieve a sufficiently realistic reproduction of the natural reduction of the link elastic oscillations [10]. The control scheme has been tested and tuned by studying the step response of the closed-loop system both for a clockwise and a counterclockwise rotation of the crank (in other words, corresponding to a square wave reference signal). The reference path that the controlled variable has to follow is characterized by a step change of 45^o taking place at time $0.1\ s$, followed by another step change of the same amplitude, but in the opposite direction, taking place after $1.5\ s$. The values of the adaptive regulator parameters have been determined so as to obtain a step response of $\theta(t)$ characterized by a short settling time and a very limited overshoot with respect to the final value, and, at the same time, an effective reduction of the amplitudes of the link elastic oscillations. For the sake of simplicity, the vibration control has been performed by resorting to the curvature of the first and the third links, while neglecting that of the second link. Due to the system configuration, this choice practically does not affect the controller performances. No optimization technique has been employed in the parameter tuning since determining the best values for the parameters is beyond the scope of this work. Table 2 reports a set of values of the controller parameters which have allowed meeting the requirements previously defined.

Table 1. Mechanical parameters of the four-bar manipulator

Link	**0**	**1**	**2**	**3**
Length $[m]$	0.360	0.373	0.525	0.632
Cross − Sectional Area $[m^2]$		$36 \cdot 10^{-6}$		
Joint	**A**	**B**	**C**	**D**
Mass $[kg]$	-	0.0724	0.0713	-
Inertia $[kgm^2]$	$490 \cdot 10^{-6}$	-	-	$120 \cdot 10^{-7}$
Flexural Stiffness $[Nm^2]$		21.6		

Table 2. Adaptive controller parameters

POSITION	**CONTROL**	**VIBRATION**	**CONTROL**
k_p	$480 \cdot 10^{-6}$	α_1	600
k_d	$130 \cdot 10^{-6}$	β_1	3
		γ_1	$2 \cdot 10^{-7}$
		α_3	6000
		β_3	1
		γ_3	$2 \cdot 10^{-7}$
		s_1	0.44
		s_3	0.5

The black lines in Fig. 2, 3 and 4 show the time-histories of the controlled variables (respectively θ, C_1 and C_3) computed carrying out the experiment with the controller parameter values set as in Table 2. The time-histories of the link curvatures are also shown in Fig. 5 and 6, where a shorter time scale is adopted for the sake of clarity. The comparison of the aforementioned time-histories with those obtained without vibration control (i.e. setting $k_1 = k_3 = 0$

and the position controller parameters as in Table 2) clearly demonstrates the effectiveness of the control scheme. In fact, when no vibration control is performed, oscillations of a not negligible amplitude are clearly visible not only in the link curvature plots, but also in the crank angle plot. Fig. 7 shows the time histories of the two adaptive gains $k_1(t)$ and $k_3(t)$, respectively. It can be noticed that both gains swiftly rise from zero when the vibrational phenomena are sensed through the curvature measurements. This behavior causes a prompt damping of the link vibrations. Then the adaptive law makes the gains gradually drop, thus causing a prominent contribution of the position regulator, until further vibrational phenomena are recorded (e.g. at time $1.6\ s$).

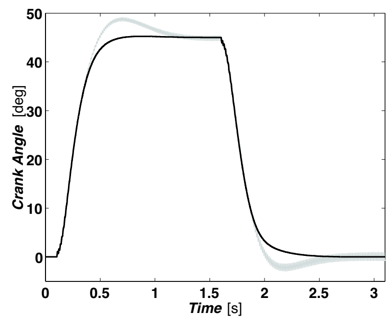

Fig. 2 Crank angles with (black line) and without (gray line) vibration control.

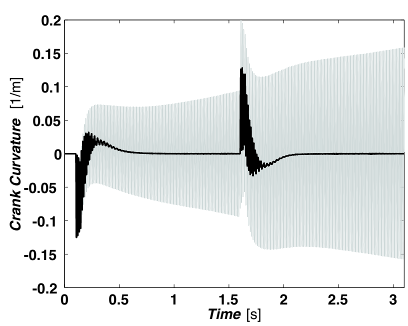

Fig. 3 Crank curvatures with (black line) and without (gray line) vibration control.

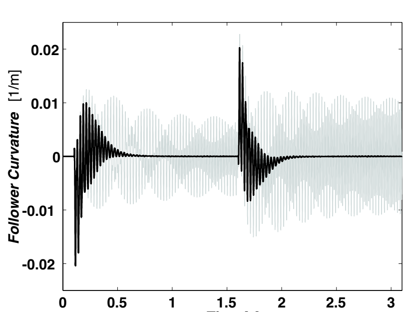

Fig. 4 Follower curvatures with (black line) and without (gray line) vibration control.

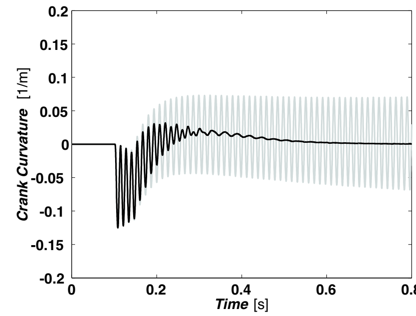

Fig. 5 Comparison of the crank curvatures, detail.

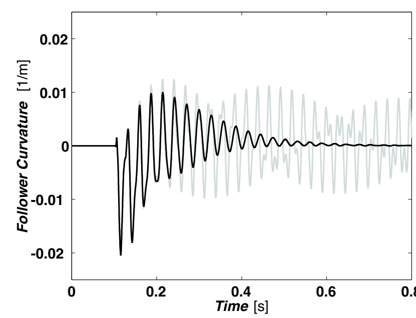

Fig. 6 Comparison of the follower curvatures, detail.

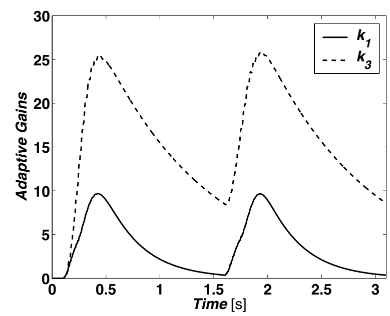

Fig. 7 Adaptive gains $k_1(t)$ and $k_3(t)$.

The superiority of the proposed adaptive scheme with respect to the corresponding non-adaptive one, which can be obtained just employing constant gains, is proved by the results reported in Fig. 8 through 11. Such figures refer to a test similar to the previous one (step response) but in which a rectangular pulse has been superimposed to the command signal so as to simulate an undesired disturbance in the control system causing improved vibrational phenomena. The pulse is applied at time $0.4\ s$, its amplitude is $3\ Nm$, and its duration $0.02\ s$. The constant gains employed in the non-adaptive scheme are the mean values of the adaptive gains computed in the previous test (Fig. 7). Their values are respectively: $k_1 = 3.838$ and $k_3 = 16.840$.

Fig. 8 proves that the adaptive scheme (black line) ensures a shorter settling time of $\theta(t)$ and a considerably lower overshoot with respect to the non-adaptive scheme (gray line). Even more, Fig. 9 and 10 show that the adaptive scheme reacts more effectively to the disturbance, allowing a much faster damping of the oscillations of the links induced by the rectangular pulse. This a consequence of the very prompt and fast rise of the adaptive gains which takes place when the pulse is applied (Fig. 11).

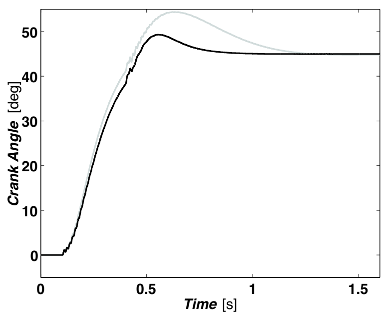

Fig. 8 Crank angles with the adaptive (black line) and the non-adaptive (gray line) control scheme.

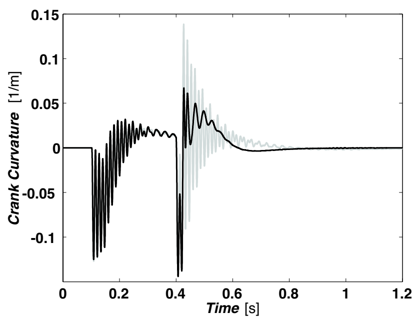

Fig. 9 Crank curvatures with the adaptive (black line) and the non-adaptive (gray line) control scheme.

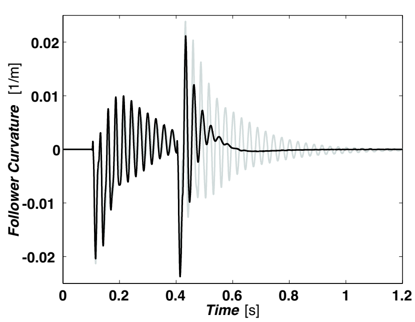

Fig. 10 Follower curvatures with the adaptive (black line) and the non-adaptive (gray line) control scheme.

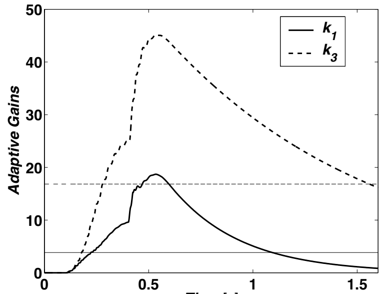

Fig. 11 $k_1(t)$ *and* $k_3(t)$ *with the adaptive and the non-adaptive control scheme.*

VII. CONCLUSIONS

This paper proposes an adaptive energy-based control strategy for multibody mechanisms with elastic links. The controller implementation has been carried out with reference to a planar four-bar flexible-link mechanism, laying on a horizontal plane. The controller has been obtained by superposing a PD position controller and an adaptive proportional vibration controller, whose (vector) gain has been adaptively tuned. The controlled-system simple stability has been proved by means of a model-independent energy-based approach. The controller performances have been illustrated by means of simulations and compared to the performances of "analogous" non-adaptive control schemes.

Both the control law and the corresponding stability analysis may be applied to a wide class of mechanical systems exhibiting undesired vibrational phaenomena: those systems whith neglible dissipative forces and for which the non-conservative forces represent the control variables.

REFERENCES

[1] R. Caracciolo, A. Gasparetto, A. Rossi and A. Trevisani, "Linear Quadratic Optimal Control of a Planar Four-Link Flexible Linkage", *Proceedings of the IASTED International Conference "Robotics and Applications 2000"*, 100-106, Honolulu, Hawaii, USA, 2000.

[2] R. Caracciolo, A. Gasparetto and A. Trevisani, "Experimental Validation of a Dynamic Model for Flexible Link Mechanisms", *Proc. of the ASME DETC 2001*, VIB-21354, Pittsburgh-USA, 2001.

[3] R. Caracciolo and A. Trevisani "Simultaneous Rigid-Body Motion and Vibration Control of a Flexible Four-Bar Linkage", *Mechanism and Machine Theory*, 36: 221-243, 2001.

[4] S.S. Ge, T.H. Lee and G. Zhu, "Energy-Based Robust Controller Design for Multi-link Flexible Robots", *Mechatronics*, 6 (7), 779-798, 1996

[5] M. Giovagnoni, "A Numerical and Experimental Analysis of a Chain of Flexible Bodies", *ASME Journal of Dynamic Systems, Measurement, and Control*, 116, 73-80, 1994.

[6] T.H. Lee, S.S. Ge and Z.P. Wang, "Adaptive Robust Controller Design for Multi-link Flexible Robots", *Mechatronics*, 11, 951-967, 2001.

[7] Z.-H. Luo and Y. Sakawa, "Gain Adaptive DSFB Control of Flexible Robot Arms", *Proceedings of the IEEE Tencon'93 Conference*, Beijing, 199-202, 1993.

[8] J.H. Park and H. Asada "Dynamic Analysis of Noncollocated Flexible Arms and Design of Torque Transmission Mechanism", *ASME Journal of Dynamic Systems, Measurement, and Control*, 116: 201-207, 1994.

[9] B. Siciliano, J.V.R. Prasad and A.J. Calise "Design of optimal output feedback compensators in two-time scale systems", *IEEE Transactions on Automatic Control*, AC-35 (4): 488-492, 1990.

[10] A. Trevisani, "Feedback Control of Flexible Four-Bar Linkages: a Numerical and Experimental Investigation", *Journal of Sound and Vibration*, 268(5): 947-970, 2003.

[11] J.H. Yang, F. Li Lian and Li Chen Fu, "Nonlinear adaptive control for flexible-link manipulators", *IEEE Transactions on Robotics and Automation*, 13 (1): 140-148, 1997.

[12] P. Zhou, F.Y. Wang, W. Chen and P. Lever, "Optimal Construction and Control of Flexible Manipulators: a Case Study Based on LQR Output Feedback", *Mechatronics*, 11: 59-77, 2001.